

---

---

# Central Benzodiazepine Receptor Binding Potential and CBF Images on SPECT Correlate with Oxygen Extraction Fraction Images on PET in the Cerebral Cortex with Unilateral Major Cerebral Artery Occlusive Disease

Kohei Chida<sup>1,2</sup>, Kuniaki Ogasawara<sup>1,2</sup>, Hiroki Kuroda<sup>1,2</sup>, Kenta Aso<sup>1,2</sup>, Masakazu Kobayashi<sup>1,2</sup>, Shunrou Fujiwara<sup>1</sup>, Kenji Yoshida<sup>1</sup>, Kazunori Terasaki<sup>2</sup>, and Akira Ogawa<sup>1,2</sup>

<sup>1</sup>Department of Neurosurgery, School of Medicine, Iwate Medical University, Morioka, Japan; and <sup>2</sup>Cyclotron Research Center, School of Medicine, Iwate Medical University, Morioka, Japan

Oxygen extraction fraction (OEF) is a key predictor of stroke recurrence in patients with symptomatic major cerebral arterial occlusive disease. The purpose of the present study was to compare central benzodiazepine receptor binding potential (BRBP) and cerebral blood flow (CBF) images on SPECT with OEF images on PET in patients with chronic unilateral middle cerebral artery (MCA) or internal carotid artery (ICA) occlusive disease. **Methods:** OEF, CBF, and BRBP were assessed using <sup>15</sup>O PET and *N*-isopropyl-*p*-<sup>123</sup>I-iodoamphetamine and <sup>123</sup>I-*l*-iomazenil SPECT, respectively, in 20 healthy subjects and in 34 patients with unilateral MCA or ICA occlusive disease. All images were transformed into the standard brain size and shape by linear and nonlinear transformation using statistical parametric mapping for anatomic standardization. A region of interest (ROI) was automatically placed according to the arterial supply using a 3-dimensional stereotactic ROI template, and the ratio of the value in the affected side to that in the contralateral side was calculated in each image. **Results:** Among patients with occlusive disease, a significant positive correlation was observed between PET OEF and SPECT BRBP/CBF ratios in 3 cerebral cortical regions ( $r = 0.851$ ,  $P < 0.0001$ , for anterior cerebral artery [ACA] ROI;  $r = 0.807$ ,  $P < 0.0001$ , for MCA ROI; and  $r = 0.774$ ,  $P < 0.0001$ , for posterior cerebral artery [PCA] ROI), but there were no correlations between these 2 parameters in the basal ganglia or the cerebellum. When an abnormally elevated PET OEF ratio was defined as a value greater than the mean + 2 SDs obtained in healthy subjects, sensitivity and specificity were, respectively, 100% and 96% for the ACA ROI, 100% and 89% for the MCA ROI, and 100% and 93% for the PCA ROI for the SPECT BRBP/CBF ratio for detecting an abnormally elevated PET OEF ratio. **Conclusion:** BRBP/CBF images on SPECT correlate with OEF images on PET in a specific clinical setting—that is, in the cerebral cortex of patients with chronic unilateral MCA or ICA occlusive disease.

**Key Words:** <sup>123</sup>I-iomazenil; cerebral blood flow; oxygen extraction fraction

**J Nucl Med 2011; 52:511–518**

DOI: 10.2967/jnumed.110.084186

**I**n the physiologic process known as cerebrovascular autoregulation, reductions in cerebral perfusion pressure can lead to compensatory dilation of precapillary resistance vessels to maintain cerebral blood flow (CBF) (1,2). However, autoregulatory capacity is not sufficient to compensate for severe reductions in cerebral perfusion pressure, and a decrease in CBF can thereby result in this context. This phenomenon is sometimes called misery perfusion (3) and leaves cerebral oxygen metabolism and brain function dependent on a progressive increase in oxygen extraction fraction (OEF) (1,4). In patients with symptomatic major cerebral arterial occlusive disease, misery perfusion increases the risk of stroke recurrence (5–7). Although identification and optimal treatment of patients with misery perfusion may therefore help to prevent stroke recurrence, direct measurement of OEF can occur only via PET. However, the clinical use of PET is precluded by its high cost and limited availability in the clinical setting.

Brain perfusion SPECT with an acetazolamide challenge is another reliable method for identifying patients with hemodynamic impairment (8,9) and those who are at high risk for stroke recurrence (10,11). However, acetazolamide is associated with a variety of frequent adverse side effects, including metabolic acidosis, hypokalemia, numbness of the extremities, headache, tinnitus, gastrointestinal disturbances, and Stevens–Johnson syndrome (12,13). Thus, it would be beneficial to develop a different method of detecting misery perfusion that does not require administration of acetazolamide.

The distribution of central benzodiazepine receptors in the cerebral cortex of the human brain has been widely studied with PET using <sup>11</sup>C-flumazenil or SPECT using

---

Received Oct. 15, 2010; revision accepted Jan. 12, 2011.  
For correspondence or reprints contact: Kuniaki Ogasawara, Department of Neurosurgery, Iwate Medical University, 19-1 Uchimaru, Morioka, 020-8505 Japan.  
E-mail: kuogasa@iwate-med.ac.jp  
COPYRIGHT © 2011 by the Society of Nuclear Medicine, Inc.

$^{123}\text{I}$ -iomazenil (14-20). Benzodiazepine receptor binding potential (BRBP) on  $^{11}\text{C}$ -flumazenil PET or  $^{123}\text{I}$ -iomazenil SPECT images is associated with neural density in the cerebral cortex, and a reduction in cortical BRBP indicates cortical neural damage or loss (14,16-20). BRBP in the cerebral cortex on  $^{11}\text{C}$ -flumazenil PET or  $^{123}\text{I}$ -iomazenil SPECT images also correlates with the cerebral cortical metabolic rate of oxygen ( $\text{CMRO}_2$ ) in patients with carotid artery occlusive disease (21,22). Because OEF is a function of  $\text{CMRO}_2/\text{CBF}$ , SPECT-defined BRBP/CBF in the cerebral cortex may correlate with OEF.

Thus, the purpose of the present study was to compare BRBP/CBF images on SPECT with OEF images on PET in the cerebral cortex, basal ganglia, and cerebellum of patients with chronic unilateral middle cerebral artery (MCA) or internal carotid artery (ICA) occlusive disease.

## MATERIALS AND METHODS

### Healthy Volunteers

The group of subjects comprised 20 healthy men, aged 30–52 y (mean age, 38 y), who underwent screening, including past medical history, physical examination, neurologic and cognitive testing, and MRI. Exclusion criteria included any history of hypertension, diabetes mellitus, atrial fibrillation, pulmonary disease, use of benzodiazepine drugs, or presence of organic brain lesions, including leukoaraiosis or asymptomatic lacunar infarction, on MRI.

### Patients

Thirty-four patients (6 women and 28 men), aged 31–74 y (mean age, 63 y), with unilateral MCA or ICA stenocclusive diseases were also included in this study. None of these patients had a history of treatment with benzodiazepine drugs, and all patients had experienced prior cerebral ischemic events. T1-, T2-, and diffusion-weighted MRI was performed in all patients, and patients with cortical infarction only were excluded. Eighteen patients had experienced transient ischemic attacks with ( $n = 10$ ) or without ( $n = 8$ ) definite cerebral border zone infarction on MRI. The remaining 16 patients had experienced minor complete strokes with definite cerebral border zone infarction on MRI. Cerebral angiography with arterial catheterization or MR angiography demonstrated ICA stenosis (>70%) in 8 patients, ICA occlusion in 14 patients, MCA stenosis (>50%) in 2 patients, and MCA occlusion in 10 patients. No patient had occlusion or stenosis of greater than 50% in the contralateral ICA or MCA.

The study protocol was approved by the local ethics committee. Written informed consent was obtained from all subjects before enrollment in the study. The total whole-body radiation doses were 1.31 or 3.81 mGy for healthy volunteers undergoing PET or SPECT, respectively, and 5.12 mGy for patients.

### Brain PET Study

PET studies were performed using a SET-3000GCT/M scanner (Shimadzu Corp.) (23). This modality uses gadolinium silica oxide detectors and provides 59 slices with 2.6-mm slice thickness. The axial field of view was 156 mm, and the spatial resolution was 3.5 mm in full width at half maximum (FWHM) at 1 cm in-plane and 4.2 mm in FWHM at center axially. The scanner was operated in a static scan mode with dual-energy window acquisition for scatter correction. The coincidence time window was set to 10 ns. A shield module consisting of 7-mm-thick lead

plates attached to the gantry bed and covering the breast and shoulder of the subject was used to reduce the counting rate of random coincidence and scatter coincidence attributable to radioactivity outside the field of view.

Before the emission scan, a transmission scan (3 min) with a  $^{137}\text{Cs}$  point source was obtained with a bismuth germanate transmission detector ring coaxially attached to the gadolinium silica oxide emission detector ring. CBF was determined while the subject continuously inhaled  $\text{C}^{15}\text{O}_2$  through a mask. Measurements of  $\text{CMRO}_2$  and OEF were obtained during continuous inhalation of  $^{15}\text{O}_2$ . Data were collected for 5 min. A single breath of  $\text{C}^{15}\text{O}$  was used to measure cerebral blood volume. CBF,  $\text{CMRO}_2$  and OEF were calculated using the steady-state method (24), and  $\text{CMRO}_2$  and OEF were corrected according to cerebral blood volume (25).

All patients underwent PET at least 1 mo after the last ischemic event.

### Brain SPECT Study

SPECT studies were performed using a ring-type SPECT scanner (Headtome-SET080; Shimadzu Corp.) (26), which provided 31 tomographic images simultaneously. The spatial resolution of the scanner with a low-energy, all-purpose collimator was 13 mm in FWHM at the center of the field of view, and the slice thickness was 25 mm in FWHM at the center of the field of view. Image slices were taken at 5-mm center-to-center spacing, parallel to the orbitomeatal line. The images were reconstructed using weighted filtered backprojection, in which the attenuation was corrected by detecting the edge of the object. An attenuation coefficient of  $0.065\text{ cm}^{-1}$ , a Butterworth filter (cutoff, 0.45 cycle/cm; order, 3), and a ramp filter were used for image reconstruction.

The distribution of CBF was assessed using *N*-isopropyl-*p*- $^{123}\text{I}$ -iodoamphetamine ( $^{123}\text{I}$ -IMP) and SPECT within 7 d after PET study. The  $^{123}\text{I}$ -IMP SPECT study was performed as described previously (26). Briefly, after a 1-min intravenous infusion of 222 MBq of  $^{123}\text{I}$ -IMP (5-mL volume) at a constant rate of 5 mL/min and a 1-min infusion of physiologic saline at the same rate, data were acquired at a midscan time of 30 min, for a scan duration of 20 min.

The distribution of BRBP in the cerebral cortex was assessed using  $^{123}\text{I}$ -iomazenil SPECT between 2 and 7 d after  $^{123}\text{I}$ -IMP SPECT study. Subjects received approximately 167 MBq of  $^{123}\text{I}$ -iomazenil by intravenous bolus injection of 1.5 mL of solution into the cubital vein. Scans (duration, 23 min) were initiated 180 min after injection because investigators have demonstrated that these images are proportional to the distribution of BRBP (16–18).

### Data Analysis

All PET and SPECT images were transformed into the standard brain size and shape by linear and nonlinear transformation using statistical parametric mapping (SPM99; Wellcome Trust Centre for Neuroimaging) for anatomic standardization (27). Thus, brain images from all subjects had the same anatomic format. In SPECT images, the ratio of radioactive counts of  $^{123}\text{I}$ -iomazenil to those of  $^{123}\text{I}$ -IMP was calculated for each pixel and was defined as BRBP/CBF. Three hundred eighteen constant regions of interest (ROIs) were automatically placed in both the cerebral and the cerebellar hemispheres using a 3-dimensional stereotactic ROI template (28). The ROIs were grouped into 12 segments (callosomarginal, pericallosal, precentral, central, parietal, angular, temporal, posterior, hippocampal, basal ganglionic, thalamic, and cerebellar) in each hemisphere, according to the arterial supply

and were summed. Then, the segments were defined as follows: callosomarginal and pericallosal segments as a cortical ROI perfused by the anterior cerebral artery (ACA); precentral, central, parietal, angular, and temporal segments as a cortical ROI perfused by the MCA; a posterior segment as a cortical ROI perfused by the posterior cerebral artery (PCA); a basal ganglionic ROI; and a cerebellar ROI (Fig. 1). The mean value was measured in each ROI on SPECT CBF, SPECT BRBP, SPECT BRBP/CBF, PET CBF, PET CMRO<sub>2</sub>, and PET OEF images. Then, the ratio of the value in the affected hemisphere to that in the contralateral hemisphere was calculated in the ACA, MCA, and PCA cortical ROIs and in the basal ganglionic ROI; the ratio of the value in the hemisphere contralateral to the affected artery to that in the ipsilateral hemisphere was calculated in the cerebellar ROI.

Healthy volunteers were assigned to 1 of 2 groups, each consisting of 10 subjects who underwent PET or SPECT study. The PET OEF ratio or SPECT BRBP/CBF ratio was calculated in each ROI when the left cerebral hemisphere or the right cerebellar hemisphere was defined as the affected side.

### Statistical Analysis

Data are expressed as the mean  $\pm$  SD. Correlations between various parameters were determined by linear regression analysis. Bland–Altman analysis was also performed to confirm concordance between variables on SPECT and those on PET (gold standard) (29). Statistical significance was set at a *P* value of less than 0.05. When the correlation between SPECT BRBP/CBF and PET OEF ratios was significant and an abnormally elevated PET OEF ratio in each region was defined as a value greater than the mean + 2 SDs obtained in healthy subjects, the accuracy of the SPECT BRBP/CBF ratio for detecting an abnormally elevated PET OEF ratio in each region in patients was determined by a receiver-operating-characteristic curve, and the area under the curve was calculated. The curve was calculated in increments or decrements of 0.5 SD from the mean value of SPECT BRBP/CBF ratios obtained in healthy subjects.

### RESULTS

SPECT CBF ratios correlated with PET CBF ratios in all 5 regions in patients with occlusive disease ( $r = 0.841$ ,  $P < 0.0001$ , for ACA cortical ROI;  $r = 0.672$ ,  $P < 0.0001$ , for MCA cortical ROI;  $r = 0.665$ ,  $P < 0.0001$ , for PCA cortical ROI;  $r = 0.718$ ,  $P < 0.0001$ , for basal ganglionic ROI; and  $r = 0.622$ ,  $P < 0.0001$ , for cerebellar ROI) (Supplemental Fig. 1; materials are available online only at <http://jnm.snmjournals.org>). However, in all 5 regions, SPECT CBF ratios showed a propensity toward overestimation at lower PET CBF ratios. No constant bias for SPECT CBF and PET CBF ratios was detected by Bland–Altman analysis in any of the 5 regions (Table 1). Although no proportional bias for the 2 ratios was observed in the ACA and MCA cortical ROIs, bias was identified in the PCA cortical, basal ganglionic, and cerebellar ROIs (Table 1).

SPECT BRBP ratios correlated with PET CMRO<sub>2</sub> ratios in 3 cortical regions ( $r = 0.776$ ,  $P < 0.0001$ , for ACA cortical ROI;  $r = 0.471$ ,  $P = 0.0044$ , for MCA cortical ROI; and  $r = 0.534$ ,  $P = 0.0009$ , for PCA cortical ROI) but not in the basal ganglia ( $r = 0.298$ ,  $P > 0.05$ ) or the



**FIGURE 1.** Diagrams showing some ROIs in 3-dimensional stereotactic ROI template. Blue ROIs (callosomarginal and pericallosal segments) indicate territories perfused by bilateral ACAs; orange ROIs (precentral, central, parietal, angular, and temporal segments) indicate territories perfused by bilateral MCAs; green ROIs (posterior segments) indicate territories perfused by bilateral PCAs; red ROIs indicate bilateral basal ganglia; and gray ROIs indicate bilateral cerebellar hemispheres.

cerebellum ( $r = -0.165$ ,  $P > 0.05$ ) in patients with occlusive disease (Supplemental Fig. 2). In the 3 cerebral cortical regions, SPECT BRBP ratios showed a propensity to overestimate values at lower PET CMRO<sub>2</sub> ratios. Although no

**TABLE 1**  
Results of Bland–Altman Analysis Between Variables in SPECT and PET

Variable	Constant bias			Proportional bias		
	Mean difference	95% confidence interval of difference	Presence or absence of bias	Slope of regression equation	<i>P</i>	Presence or absence of bias
<b>SPECT CBF vs. PET CBF ratios</b>						
ACA cortical ROI	−0.011	−0.085 to 0.064	Absence	−0.125	0.2371	Absence
MCA cortical ROI	−0.002	−0.158 to 0.155	Absence	−0.194	0.2204	Absence
PCA cortical ROI	−0.014	−0.142 to 0.115	Absence	−0.347	0.0321	Presence
Basal ganglionic ROI	0.022	−0.180 to 0.224	Absence	−0.410	0.0056	Presence
Cerebellar ROI	−0.047	−0.213 to 0.119	Absence	−0.410	0.0182	Presence
<b>SPECT BRBP vs. PET CMRO<sub>2</sub> ratios</b>						
ACA cortical ROI	−0.009	−0.084 to 0.067	Absence	−0.378	0.0039	Presence
MCA cortical ROI	0.027	−0.128 to 0.183	Absence	−0.638	0.0027	Presence
PCA cortical ROI	−0.004	−0.133 to 0.125	Absence	−0.831	<0.0001	Presence
Basal ganglionic ROI	—	—	—	—	—	—
Cerebellar ROI	—	—	—	—	—	—
<b>SPECT BRBP/CBF vs. PET OEF ratios</b>						
ACA cortical ROI	−0.024	−0.105 to 0.058	Absence	−0.021	0.8340	Absence
MCA cortical ROI	0.042	−0.062 to 0.147	Absence	−0.170	0.1482	Absence
PCA cortical ROI	0.018	−0.059 to 0.094	Absence	−0.060	0.6388	Absence
Basal ganglionic ROI	—	—	—	—	—	—
Cerebellar ROI	—	—	—	—	—	—

constant bias for SPECT BRBP ratios and PET CMRO<sub>2</sub> ratios was detected by Bland–Altman analysis in the 3 cortical regions, proportional bias for the 2 ratios was identified in the 3 cortical regions (Table 1).

SPECT BRBP/CBF ratios correlated with PET OEF ratios in 3 cortical regions ( $r = 0.851$ ,  $P < 0.0001$ , for ACA cortical ROI;  $r = 0.807$ ,  $P < 0.0001$ , for MCA cortical ROI; and  $r = 0.774$ ,  $P < 0.0001$ , for PCA cortical ROI) but not in the basal ganglia ( $r = 0.320$ ,  $P > 0.05$ ) or in the cerebellum ( $r = -0.243$ ,  $P > 0.05$ ) in patients with occlusive disease (Fig. 2 and Supplemental Fig. 3). Again, in the 3 cortical regions, SPECT BRBP/CBF ratios showed a propensity toward overestimation at lower PET OEF ratios. No constant or proportional bias for SPECT BRBP/CBF and PET OEF ratios was detected by Bland–Altman analysis in the 3 cortical regions (Table 1).

The PET OEF and SPECT BRBP/CBF ratios in healthy subjects were  $1.001 \pm 0.045$  and  $1.001 \pm 0.051$  for the ACA cortical ROI,  $1.001 \pm 0.044$  and  $1.001 \pm 0.050$  for the MCA cortical ROI,  $1.002 \pm 0.045$  and  $1.001 \pm 0.052$  for the PCA cortical ROI,  $1.000 \pm 0.047$  and  $1.001 \pm 0.053$  for the basal ganglionic ROI, and  $1.000 \pm 0.045$  and  $1.000 \pm 0.050$  for the cerebellar ROI.

When an abnormally elevated PET OEF ratio was defined as a value greater than the mean + 2 SDs obtained in healthy subjects (1.091 for the ACA cortical ROI, 1.089 for the MCA cortical ROI, and 1.092 for the PCA cortical ROI), 6 and 28 patients for the ACA cortical ROI, 6 and 28 patients for the MCA cortical ROI, and 4 and 30 patients for the PCA cortical ROI were classified as having an abnormally elevated PET OEF ratio and a normal PET OEF ratio, respectively. The sensitivity and specificity for the SPECT BRBP/CBF ratio in the cutoff point lying close

to the left upper corner of the receiver-operating-characteristic curve for detection of an abnormally elevated PET OEF ratio was 100% (6/6) and 96% (27/28) (cutoff point, 1.103) for the ACA cortical ROI, 100% (6/6) and 89% (25/28) (cutoff point, 1.101) for the MCA cortical ROI, and 100% (4/4) and 93% (28/30) (cutoff point, 1.105) for the PCA cortical ROI, respectively (Fig. 2). Positive and negative predictive values were 86% (6/7) and 100% (27/27) for the ACA cortical ROI, 67% (6/9) and 100% (25/25) for the MCA cortical ROI, and 67% (4/6) and 100% (28/28) for the PCA cortical ROI, respectively, using the same cutoff point. The cutoff point for the SPECT BRBP/CBF ratio in all 3 cerebral cortical ROIs was the mean + 2 SDs of the control value obtained from healthy subjects. The area under the receiver-operating-characteristic curve was 0.992 for the ACA cortical ROI, 0.982 for the MCA cortical ROI, and 0.975 for the PCA cortical ROI.

When an abnormally elevated PET OEF ratio was defined as a value greater than the mean + 2 SDs obtained in the cerebellum of healthy subjects (1.090), none of the patients was classified as having an abnormally elevated PET OEF ratio (Supplemental Fig. 3).

Representative MR, PET, and SPECT images for a patient with unilateral ICA occlusion and an abnormally elevated PET OEF ratio are shown in Figure 3 and Supplemental Figure 4.

## DISCUSSION

The present study demonstrated that BRBP/CBF images on SPECT correlate with OEF images on PET in the cerebral cortex of patients with chronic unilateral MCA or ICA occlusive disease.

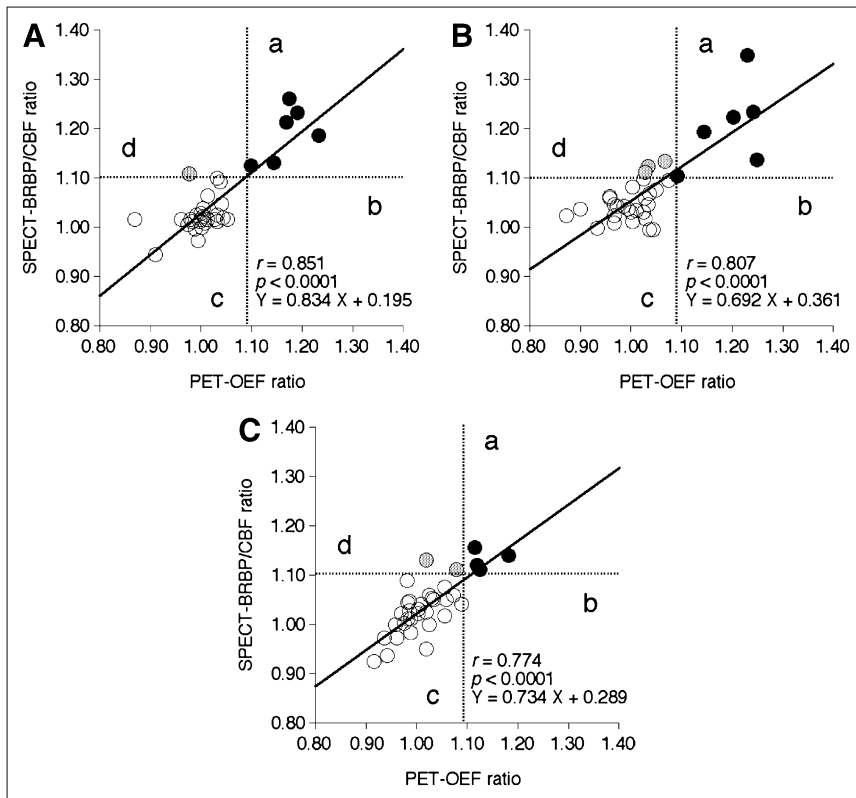


**FIGURE 2.** Correlation between SPECT BRBP/CBF and PET OEF ratios in 34 patients. (A) ACA cortical ROI. (B) MCA cortical ROI. (C) PCA cortical ROI. Plot of relationship between these 2 values reveals 4 groups of results: those with elevated SPECT BRBP/CBF ratios and elevated PET OEF ratios (true-positive; ●) (a), those with only elevated PET OEF ratios (false-negative; there is no case with this outcome) (b), those without elevated SPECT BRBP/CBF ratios and elevated PET OEF ratios (true-negative; ○) (c), and those with only elevated SPECT BRBP/CBF ratios (false-positive; half-tone circle) (d). Dashed horizontal and vertical lines denote mean + 2 SDs of SPECT BRBP/CBF and PET OEF ratios obtained in healthy volunteers, respectively.

In the present study, SPECT BRBP ratios correlated with PET CMRO<sub>2</sub> ratios in the cerebral cortex, consistent with previous findings (21). Yamauchi et al. (14) measured central BRBP with PET using <sup>11</sup>C-flumazenil in patients with ICA chronic occlusive disease and concluded that selective neuronal damage reflected by decreased BRBP in the cerebral cortex is associated with border zone infarction, suggesting that chronic hemodynamic ischemia leading to border zone infarction may cause selective neuronal damage in the normal-appearing cerebral cortex beyond the regions of infarcts. In such cerebral cortex, CMRO<sub>2</sub> probably reduces with the degree of neuronal damage (21), resulting in a correlation between SPECT BRBP and PET CMRO<sub>2</sub> ratios.

By contrast, no significant correlation was observed between SPECT BRBP and PET CMRO<sub>2</sub> ratios in the basal ganglia. One possible explanation for these data involves the normal regional distribution of SPECT BRBP. The rank order of the SPECT BRBP ratios in the human brain is cerebral cortex >> basal ganglia (30–32), and this order is similar to the rank order of benzodiazepine receptor densities observed in in vitro benzodiazepine receptor autoradiographic studies using human brain tissue (33–35). Thus, the considerably lesser benzodiazepine receptor densities might reduce the affected side-to-contralateral side asymmetry of SPECT BRBP in the basal ganglia. No significant correlation was observed between SPECT BRBP and PET CMRO<sub>2</sub> ratios in the cerebellum. Several investigators have demonstrated that the cerebellar accumulation of <sup>123</sup>I-ioma-

zenil is symmetric when CBF and CMRO<sub>2</sub> in the cerebellar hemisphere contralateral to the lesion in the cerebral hemisphere are reduced as a result of crossed cerebellar diaschisis (18,21,36). On the basis of these findings, those investigators concluded that the <sup>123</sup>I-iomazenil SPECT images are not influenced by a reduction of the brain metabolism due to the remote effect if the neural tissues are viable (18,21). This conclusion is consistent with observations from the present study, in which there was no correlation between SPECT BRBP and PET CMRO<sub>2</sub> ratios in the cerebellum.

Although SPECT BRBP ratios correlated with PET CMRO<sub>2</sub> ratios in the 3 cortical regions in the present study, SPECT BRBP ratios were overestimated at lower PET CMRO<sub>2</sub> ratios in those regions. This overestimation was even greater than that seen for the SPECT CBF ratios at lower PET CBF ratios, suggesting that overestimation of SPECT BRBP ratios may be due to other factors in addition to errors in SPECT reconstruction. Three cerebral cortical ROIs on the 3-dimensional stereotactic ROI template used in the present study include not only the cerebral cortex but also the cerebral white matter (28). According to previous <sup>123</sup>I-iomazenil SPECT and in vitro autoradiographic studies in humans, benzodiazepine receptor density is considerably lower in the cerebral white matter than in the cerebral cortex (30,31). The contamination of the white matter with low BRBP in the cerebral cortical ROIs may thus reduce the affected side-to-contralateral side asymmetry of SPECT BRBP, resulting in the overestimation of SPECT BRBP



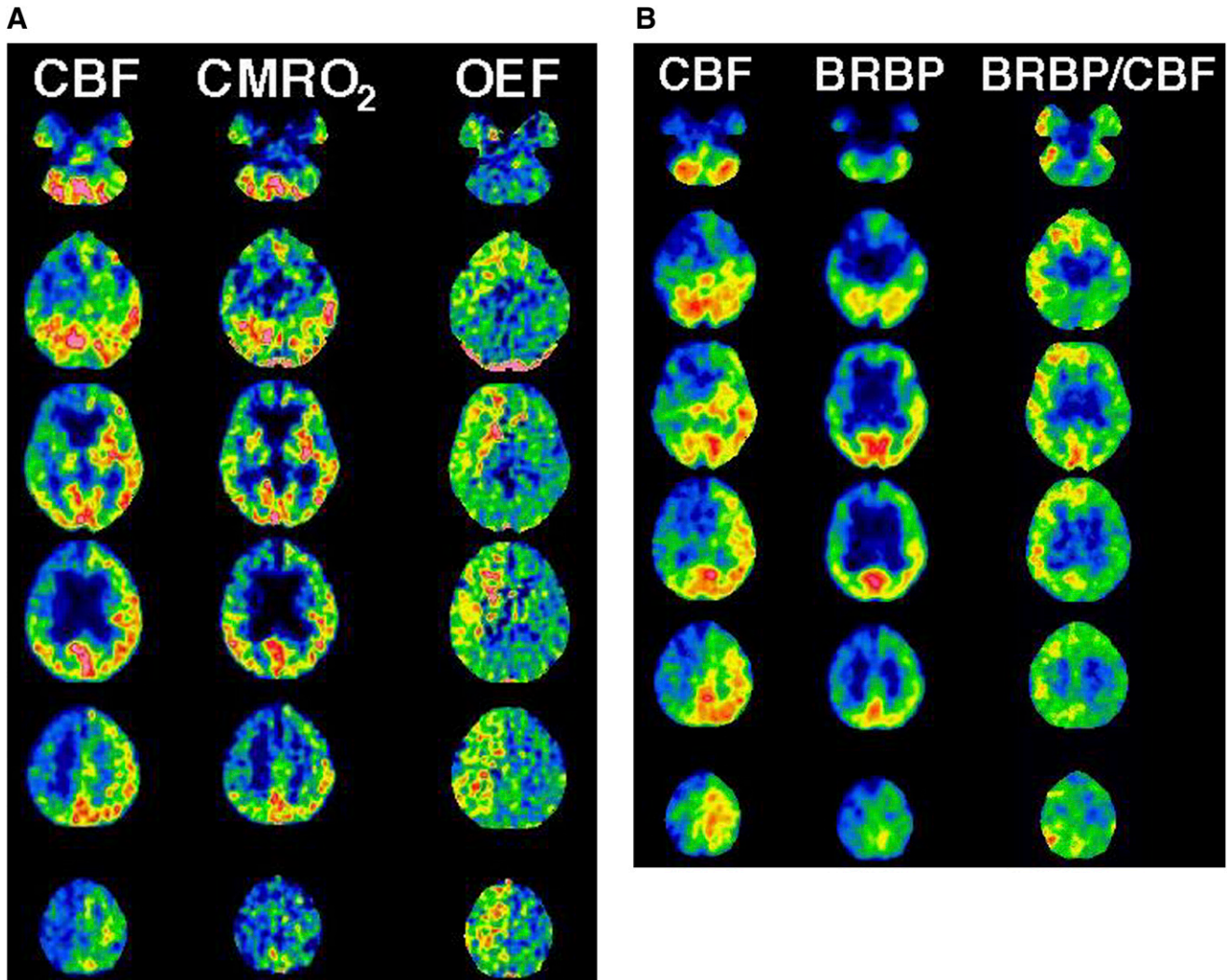


**FIGURE 3.** A 69-y-old man with right ICA occlusion and transient ischemic attack manifesting as left motor weakness. (A) PET shows severely reduced CBF, slightly reduced  $CMRO_2$ , and elevated OEF in right cerebral hemisphere when compared with left cerebral hemisphere. (B) *N*-isopropyl- $p$ - $^{123}I$ -iodoamphetamine and  $^{123}I$ -iomazenil SPECT show severely reduced CBF and slightly reduced BRBP, respectively, in right cerebral hemisphere when compared with left cerebral hemisphere. As a result, BRBP/CBF ratios are relatively increased in right cerebral hemisphere.

ratios. Further, metabolism in the cerebral cortex with border zone infarction may be reduced because of a remote effect from the infarction in addition to selective neuronal damage. BRBPs are not influenced by a reduction of the brain metabolism due to the remote effect if the neural tissues are viable (18,21). As a result, the reduction in BRBP may be less than that in  $CMRO_2$  in the cerebral cortex with border zone infarction, which also leads to overestimation of SPECT BRBP ratios.

Although there was no correlation between SPECT BRBP/CBF and PET OEF ratios in the basal ganglia and cerebellum, a strong positive correlation between the two was observed in the cerebral cortical ROIs, even despite the fact that SPECT BRBP/CBF ratios were overestimated at lower PET OEF ratios in those regions. These findings may be related to the correlation between SPECT BRBP and PET  $CMRO_2$  ratios in each region and the overestimation

of the SPECT BRBP ratio as the PET  $CMRO_2$  ratio decreases. In addition, none of patients was classified as having an abnormally elevated PET OEF ratio in the cerebellum. Matched perfusion in crossed cerebellar diaschisis might account for these data that led to a limited range of PET OEF ratio in these patients and may have contributed to the absence of correlation between SPECT BRBP/CBF and PET OEF ratios in the cerebellum.

The present study also demonstrated that SPECT BRBP/CBF ratios in the cerebral cortical ROIs provided 100% sensitivity and 89%–96% specificity, with 67%–86% positive and 100% negative predictive values for detecting abnormally elevated PET OEF ratios. The positive predictive value indicates that when patients are diagnosed with abnormally elevated SPECT BRBP/CBF ratios in the affected cerebral hemisphere, results should be confirmed with PET. By contrast, the negative predictive value indi-

cates that the present method can be used as a screening test and thereby eliminates the need for the PET study in more than half of patients (70%–80% in our study).

In this study, an abnormally elevated PET OEF ratio in the cerebral cortex was defined as a value greater than the mean + 2 SDs obtained in healthy subjects (1.089–1.092). Grubb et al. have categorized patients with a PET OEF ratio greater than 1.082 due to unilateral ICA stenocclusive disease as having misery perfusion and reported that such patients are at high risk for subsequent stroke when treated medically (7). In contrast, Yamauchi et al. reported that an increase in absolute OEF value is a better predictor of recurrent ischemic stroke than OEF asymmetry in patients with ICA or MCA stenocclusive disease including bilateral lesions (6). In fact, increased absolute OEF is an independent predictor of subsequent strokes (5,6), and the risk of stroke tends to be higher in patients with OEF asymmetry than in those without OEF asymmetry, although this difference does not reach the level of statistical significance (6). In the present study, only patients with unilateral ICA or MCA stenocclusive disease were included, and the cut-off point for the PET OEF ratio was approximately identical to that defined by Grubb et al. (7) Thus, our results suggest that BRBP/CBF images on SPECT can predict a higher risk of stroke recurrence in patients with unilateral ICA or MCA stenocclusive disease.

The present study possesses several limitations that require discussion. First, the study population included only patients with unilateral ICA or MCA occlusive disease and used affected side-to-contralateral side asymmetry on PET or SPECT images to detect misery perfusion in the affected cerebral hemisphere. However, impairments in cerebral hemodynamics are more severe in patients with bilateral major cerebral artery occlusive disease than in those with unilateral major cerebral artery occlusive disease (37), and impairments in bilateral cerebral hemodynamics in patients with bilateral major cerebral arterial occlusive disease may not be detected by the present SPECT method using affected side-to-contralateral side asymmetry. Further, even in patients with increased OEF in the ipsilateral cerebral cortex due to unilateral MCA occlusion, the OEF value may be increased in the territory of the contralateral MCA, although the latter value is less than the former value (38). Although absolute quantification of BRBP and CBF using SPECT has been reported (15,26,28), this issue of whether BRBP/CBF values quantified by these methods in patients with unilateral ICA or MCA occlusive disease and bilateral lesions correlate with OEF quantified by PET remains unclear. Further, the present study included patients with cerebral border zone infarction and excluded those with only cortical infarction, to enroll patients with cerebral ischemia due to hemodynamic mechanisms rather than to embolic or thrombotic mechanisms. Thus, the present results may not apply to patients with cortical infarction alone. Last, because  $^{123}\text{I}$ -IMP and  $^{123}\text{I}$ -iomazenil are currently unavailable in Western countries because of

cost, the merit of the present SPECT method using these tracers may be limited. However, the present study suggested that when a new SPECT tracer, whose distribution in the brain correlates with neural density or cerebral metabolism, becomes available in those countries in the future, SPECT images using the new tracer and a brain perfusion  $^{99\text{m}}\text{Tc}$  tracer (39) can be a surrogate for OEF images on PET.

## CONCLUSION

The present study demonstrated that BRBP/CBF images on SPECT correlate with OEF images on PET in a specific clinical setting—that is, in the cerebral cortex of patients with chronic unilateral MCA or ICA occlusive disease. Further investigation regarding the relationship between the BRBP/CBF images on SPECT and the risk of stroke recurrence in patients with symptomatic major cerebral artery occlusive disease would be of beneficial.

## DISCLOSURE STATEMENT

The costs of publication of this article were defrayed in part by the payment of page charges. Therefore, and solely to indicate this fact, this article is hereby marked “advertisement” in accordance with 18 USC section 1734.

## REFERENCES

1. Gibbs JM, Wise RJ, Leenders KL, Jones T. Evaluation of cerebral perfusion reserve in patients with carotid-artery occlusion. *Lancet*. 1984;1:310–314.
2. Powers WJ, Raichle ME. Positron emission tomography and its application to the study of cerebrovascular disease in man. *Stroke*. 1985;16:361–376.
3. Baron JC, Boussier MG, Rey A, Guillard A, Comar D, Castaigne P. Reversal of focal “misery-perfusion syndrome” by extra-intracranial arterial bypass in hemodynamic cerebral ischemia: a case study with  $^{15}\text{O}$  positron emission tomography. *Stroke*. 1981;12:454–459.
4. Powers WJ. Cerebral hemodynamics in ischemic cerebrovascular disease. *Ann Neurol*. 1991;29:231–240.
5. Yamauchi H, Fukuyama H, Nagahama Y, et al. Evidence of misery perfusion and risk for recurrent stroke in major cerebral arterial occlusive diseases from PET. *J Neurol Neurosurg Psychiatry*. 1996;61:18–25.
6. Yamauchi H, Fukuyama H, Nagahama Y, et al. Significance of increased oxygen extraction fraction in 5-year prognosis of major cerebral arterial occlusive diseases. *J Nucl Med*. 1999;40:1992–1998.
7. Grubb RL Jr, Derdeyn CP, Fritsch SM, et al. Importance of hemodynamic factors in the prognosis of symptomatic carotid occlusion. *JAMA*. 1998;280:1055–1060.
8. Nemoto EM, Yonas H, Kuwabara H, et al. Identification of hemodynamic compromise by cerebrovascular reserve and oxygen extraction fraction in occlusive vascular disease. *J Cereb Blood Flow Metab*. 2004;24:1081–1089.
9. Yamauchi H, Okazawa H, Kishibe Y, Sugimoto K, Takahashi M. Oxygen extraction fraction and acetazolamide reactivity in symptomatic carotid artery disease. *J Neurol Neurosurg Psychiatry*. 2004;75:33–37.
10. Kuroda S, Houkin K, Kamiyama H, Mitsumori K, Iwasaki Y, Abe H. Long-term prognosis of medically treated patients with internal carotid or middle cerebral artery occlusion: can acetazolamide test predict it? *Stroke*. 2001;32:2110–2116.
11. Ogasawara K, Ogawa A, Yoshimoto T. Cerebrovascular reactivity to acetazolamide and outcome in patients with symptomatic internal carotid or middle cerebral artery occlusion: a xenon-133 single-photon emission computed tomography study. *Stroke*. 2002;33:1857–1862.
12. Derick RJ. Carbonic anhydrase inhibitors. In: Mauger TF, Craig EL, eds. *Hevener's Ocular Pharmacology*. 6th ed. St Louis, MO: CV Mosby Co.;1994: chap. 4.
13. Ogasawara K, Tomitsuka N, Kobayashi M, et al. Stevens-Johnson syndrome associated with intravenous acetazolamide administration for evaluation of cerebrovascular reactivity: case report. *Neurol Med Chir (Tokyo)*. 2006;46:161–163.

14. Yamauchi H, Kudoh T, Kishibe Y, Iwasaki J, Kagawa S. Selective neuronal damage and borderzone infarction in carotid artery occlusive disease: a <sup>11</sup>C-flumazenil PET study. *J Nucl Med.* 2005;46:1973–1979.
15. Millet P, Graf C, Moulin M, Ibanez V. SPECT quantification of benzodiazepine receptor concentration using a dual-ligand approach. *J Nucl Med.* 2006;47:783–792.
16. Nakagawara J, Sperling B, Lassen NA. Incomplete brain infarction of reperfused cortex may be quantitated with iomazenil. *Stroke.* 1997;28:124–132.
17. Hatazawa J, Satoh T, Shimosegawa E, et al. Evaluation of cerebral infarction with iodine 123-iomazenil SPECT. *J Nucl Med.* 1995;36:2154–2161.
18. Hatazawa J, Shimosegawa E, Satoh T, Kanno I, Uemura K. Central benzodiazepine receptor distribution after subcortical hemorrhage evaluated by means of [<sup>123</sup>I]iomazenil and SPECT. *Stroke.* 1995;26:2267–2271.
19. Guadagno JV, Jones PS, Aigbirhio FI, et al. Selective neuronal loss in rescued penumbra relates to initial hypoperfusion. *Brain.* 2008;131:2666–2678.
20. Yamauchi H, Nishii R, Higashi T, Kagawa S, Fukuyama HJ. Silent cortical neuronal damage in atherosclerotic disease of the major cerebral arteries. *J Cereb Blood Flow Metab.* 2011;31:953–961.
21. Dong Y, Fukuyama H, Nabatame H, Yamauchi H, Shibasaki H, Yonekura Y. Assessment of benzodiazepine receptors using iodine-123-labeled iomazenil single-photon emission computed tomography in patients with ischemic cerebrovascular disease: a comparison with PET study. *Stroke.* 1997;28:1776–1782.
22. Yamauchi H, Nishii R, Higashi T, Kagawa S, Fukuyama H. Selective neuronal damage and Wisconsin Card Sorting Test performance in atherosclerotic occlusive disease of the major cerebral artery. *J Neurol Neurosurg Psychiatry.*, in press.
23. Ibaraki M, Miura S, Shimosegawa E, et al. Quantification of cerebral blood flow and oxygen metabolism with 3-dimensional PET and <sup>15</sup>O: validation by comparison with 2-dimensional PET. *J Nucl Med.* 2008;49:50–59.
24. Frackowiak RS, Lenzi GL, Jones T, Heather JD. Quantitative measurement of regional cerebral blood flow and oxygen metabolism in man using <sup>15</sup>O and positron emission tomography: theory, procedure, and normal values. *J Comput Assist Tomogr.* 1980;4:727–736.
25. Lammertsma AA, Jones T. Correction for the presence of intravascular oxygen-15 in the steady-state technique for measuring regional oxygen extraction ratio in the brain: 1. Description of the method. *J Cereb Blood Flow Metab.* 1983;3:416–424.
26. Ogasawara K, Ito H, Sasoh M, et al. Quantitative measurement of regional cerebrovascular reactivity to acetazolamide using [<sup>123</sup>I]iodoamphetamine autoradiographic method with single photon emission computed tomography: validation study using [<sup>15</sup>O] H<sub>2</sub>O positron emission tomography. *J Nucl Med.* 2003;44:520–525.
27. Friston KJ, Frith CD, Liddle PF, Dolan RJ, Lammertsma AA, Frackowiak RS. The relationship between global and local changes in PET scans. *J Cereb Blood Flow Metab.* 1990;10:458–466.
28. Takeuchi R, Matsuda H, Yoshioka K, Yonekura Y. Cerebral blood flow SPET in transient global amnesia with automated ROI analysis by 3DSRT. *Eur J Nucl Med Mol Imaging.* 2004;31:578–589.
29. Bland JM, Altman DG. Statistical methods for assessing agreement between two methods of clinical measurement. *Lancet.* 1986;1:307–310.
30. Bremner JD, Baldwin R, Horti A, et al. Quantitation of benzodiazepine receptor binding with PET [<sup>11</sup>C]iomazenil and SPECT [<sup>123</sup>I]iomazenil: preliminary results of a direct comparison in healthy human subjects. *Psychiatry Res.* 1999;91:79–91.
31. Woods SW, Seibyl JP, Goddard AW, et al. Dynamic SPECT imaging after injection of the benzodiazepine receptor ligand [<sup>123</sup>I]iomazenil in healthy human subjects. *Psychiatry Res.* 1992;45:67–77.
32. Busatto GF, Pilowsky LS, Costa DC, Ell PJ, Lingford-Hughes A, Kerwin RW. In vivo imaging of GABA<sub>A</sub> receptors using sequential whole-volume iodine-123 iomazenil single-photon emission tomography. *Eur J Nucl Med.* 1995;22:12–16.
33. Braestrup C, Albrechtsen R, Squires RF. High densities of benzodiazepine receptors in human cortical areas. *Nature.* 1977;269:702–704.
34. Richards JG, Möhler H. Benzodiazepine receptors. *Neuropharmacology.* 1984;23:233–242.
35. Zezula J, Cortes R, Probst A, Palacios JM. Benzodiazepine receptor sites in the human brain: autoradiographic mapping. *Neuroscience.* 1988;25:771–795.
36. Baron JC, Bousser MG, Comar D, Soussaline F, Castaigne P. ‘Crossed cerebellar diaschisis’: a remote functional suppression secondary to supratentorial infarction in man [abstract]. *J Cereb Blood Flow Metab.* 1981;1:s500.
37. Reinhard M, Muller T, Roth M, Guschlbauer B, Timmer J, Hetzel A. Bilateral severe carotid artery stenosis or occlusion: cerebral autoregulation dynamics and collateral flow patterns. *Acta Neurochir (Wien).* 2003;145:1053–1060.
38. Tanaka M, Shimosegawa E, Kajimoto K, et al. Chronic middle cerebral artery occlusion: a hemodynamic and metabolic study with positron-emission tomography. *AJNR.* 2008;29:1841–1846.
39. Ito H, Inoue K, Goto R, et al. Normal database of cerebral blood flow measured by SPECT with I-123-IMP, Tc-99m-HMPAO, and Tc-99m-ECD and PET with O-15 labeled water in humans: comparison with voxel-based morphometry [abstract]. *J Cereb Blood Flow Metab.* 2005;25:S330.